

Investigation of Space Charge Interactions Which Arise During Simultaneous Confinement of Positive and Negative Ions in an Ion Trap Mass Spectrometer

J.-C. Mathurin,¹ S. Grégoire,¹ A. Brunot,¹ J.-C. Tabet,^{1*} R. E. March,² S. Catinella³ and P. Traldi³

¹ Laboratoire de Chimie Structurale Organique et Biologique, CNRS (EP 103), Université Pierre et Marie Curie, 4 Place Jussieu, 75270 Paris Cedex 05, France

² Department of Chemistry, Trent University, Peterborough, ON, K9J 7B8, Canada

³ CNR, Area della Ricerca, Corso Stati Uniti 4, I-35020 Padova, Italy

While positive and negative ions are created simultaneously in a quadrupole ion trap during electron ionization, there is a marked preponderance of the former species. With prolonged ionization and a relatively high concentration of substrate molecules, positive ion species of low mass/charge ratio can give rise to space charge potentials that can neutralize and exceed the normal trapping potentials for positive ions of high mass/charge ratio, leading to the ejection of positive ions, but not negative ions, from the ion trap. The onset of space charge is manifested by the ejection of positive ions of $m/z > 600$; as the space charge potential is increased incrementally, ejection of positive ions is extended to those of lower mass/charge ratio, that is, to $m/z \approx 300$. Negative ions are not affected by the space charge induced by the positive ions; within the limits of experimentation, negative ions in the mass/charge ratio range m/z 352–633 remain confined within the ion trap and can be ejected during a normal analytical scan. Under the influence of positive ion-induced space charge, there is an enhancement of the storage of negative ions having low values of the trapping parameter q_z . These observations can be rationalized using a theoretical approach based on a pseudo-potential well model. Although not investigated here, the simultaneous storage of positive ions and negative ions permits the interactions between these species to be studied. © 1997 by John Wiley & Sons, Ltd

J. Mass Spectrom. 32, 829–837 (1997)

No. of Figs: 9 No. of Tables: 2 No. of Refs: 39

KEYWORDS: negative ions; space charge interactions; ion trap; ion trap mass spectrometer

INTRODUCTION

Over the past 20 years, gas chromatography combined with mass spectrometry (GC/MS) has been used widely for organic compound identification and trace detection. Electron ionization (EI) of most compounds leads to the formation of both molecular and several fragment ion species; while the resulting fragmentation patterns can serve to identify compounds, the distribution of total charge amongst several ion species can adversely affect the sensitivity of GC/MS. This disadvantage can often be overcome by using chemical ionization (CI), in which stable quasi-molecular ions are formed in relatively high abundance, free of fragment ions and more suitable for analytical purposes. Much analytical interest has been expressed in the sensitivity of negative ion chemical ionization (NICI)¹ since molecular and quasi-molecular negative ions can be generated efficiently in CI sources.

Frequently, these molecular and quasi-molecular negative ion species are stable with respect to fragmentation since they are formed in reactions of low exothermicity and, for this reason, NICI is referred to as a 'soft' ionization mode; this mode is very useful in the environmental domain² for the determination of halogenated compounds and pesticides. Negative ions are produced either directly by thermal-electron capture or, in ion-molecule reactions,³ by electron transfer, proton transfer and anion attachment. When NICI is combined with conventional tandem mass spectrometry (MS/MS), a dramatic increase in specificity and stereospecificity can be observed.⁴

Recently, the development of GC/MS (and GC/MS/MS) using an ion trap mass spectrometer^{5,6} as the mass-selective (and tandem mass-selective) detector has culminated in the realization of an instrument of high sensitivity and high specificity for organic compound analysis.⁷ Despite the relatively low capital cost of this type of bench-top instrument, both EI and low-pressure CI (with a mass-selected CI reagent ion) modes are available. As a result of recent ion trap software developments, it is possible now to customize successive mass spectrometric protocols,^{8–10} or scan functions, so as to carry out multiple mass-selective operations, (MS)ⁿ, using a series of different scan functions pro-

* Correspondence to: J.-C. Tabet, Laboratoire de Chimie Structurale Organique et Biologique, CNRS (EP 103), Université Pierre et Marie Curie, 4 Place Jussieu, 75270 Paris Cedex 05, France.

Contract grant sponsor: Centre d'Etudes du Bouchet.

Contract grant sponsor: Université Pierre et Marie Curie.

Contract grant sponsor: CNRS.

grammed to the elution time. While negative ions are produced within the quadrupole ion trap during the EI episode, such ions have not been studied extensively and few reports on negative ions have been published.^{11–17}

The formation of negative ions in the ion trap under high-frequency field conditions is a process with a very low yield relative to those of positive ions and of accompanying secondary quasi-thermal electrons. The low yield of negative ions can be attributed to a small fraction of quasi-thermal electrons which remain in the ion trap and possess low kinetic energies in the range $<1\text{--}2$ eV. Only a few electrons survive the accelerating effects of the storage potential applied to the ring electrode that normally causes electrons to be ejected rapidly,^{13,15} thus negative ion formation is severely hindered. McLuckey and co-workers¹⁸ have shown that, under EI conditions, the abundance of negative ions formed was only 10^{-3} times that of positive ions. Nascent negative ions suffer recombination in ion–ion reactions in which positive and negative ions form neutral species.^{13,19,20} Consequently, in order to study the reactivity of negative ions in the ion trap, it is normally necessary that such species be formed in an external source and injected subsequently into the ion trap.^{21–24}

In the present work, in which perfluorotributylamine (FC-43) was used as the sample molecule, negative ions were formed *in situ* by resonant electron capture under conditions of high analyte pressure within the ion trap. During the ionization period, negative ions are not isolated from the preponderance of positive ions formed. The high density of positive ions, created and stored during prolonged ionization, induces a repulsive coulombic force that gives rise to space charge perturbations; such perturbations have been studied by several workers.^{25–31} Space charge perturbations result in the destabilization of the trajectories of positive ions such that, as the magnitude of the space charge perturbation increases, positive ions are ejected in order of descending mass/charge ratio. A simple rationalization of trajectory destabilization based on the neutralization of the trapping potential is presented here.

Neutralization of the trapping potentials is effected by high densities of ions of low mass/charge ratio that are in the majority and leads to the ejection of ions of higher mass/charge ratio. This discrimination against ions of higher mass/charge ratio permits artifact-free observation of negative ions. At the same time, the space charge potential created by the positive ions of low mass/charge ratio may be responsible, as proposed in the present work, for enhanced storage in the ion trap of negative ions having a q_z value of <0.02 , where q_z is the trapping parameter.

EXPERIMENTAL

All data were acquired using a Varian Saturn III gas chromatograph/mass spectrometer equipped with a normal channeltron detector which lacked a conversion dynode normally employed for the detection of negative ions. In the present work, the gas chromatograph was

not used; rather, perfluorotributylamine was introduced into the vacuum chamber *via* a metered needle valve and a solenoid valve at a constant pressure of 7.5×10^{-6} Torr (1 Torr = 133.3 Pa) as measured with an Alcatel CF2P Penning gauge. The gauge was located on the lower part of the manifold and was not calibrated. FC-43 was obtained from Scientific Instrument Services. Helium was used as a buffer gas at an uncorrected pressure of 3×10^{-5} Torr. The manifold was maintained at a temperature of 170°C . In Fig. 1 is shown the scan function employed for EI and for the detection of positive ions and negative ions; the mass range is given for each of the four analytical scan segments.

Experiments were carried out with an r.f. storage voltage amplitude such that the low-mass cut-off (LMCO) was m/z 35, except where stated otherwise. The mass scan rate was 5555 Th s^{-1} . Axial modulation at $4 \text{ V}_{\text{p-p}}$ was used for the analytical scan of positive and negative ions. The filament emission current (FEC) was varied from 0 to $50 \mu\text{A}$ and the duration of ionization was maintained at 25 ms.

Negative ions were detected without instrument modification. In the ejection from the ion trap of ions in order of increasing mass/charge ratio during a mass-selective instability scan, ions pass through perforations in each end-cap electrode as the r.f. amplitude, V_{0-p} , is ramped. That ions emerge from the end-cap electrodes with kinetic energies proportional to V_{0-p} is not surprising; however, as the most probable kinetic energy, KE_{mp} , of an ion of mass-charge ratio m/z is $\sim 6.7ze(V_{0-p} - 200)/m$, where e is the electronic charge, the sheer magnitude of these kinetic energies is astonishing; KE_{mp} ranges from 450 eV for m/z 100 to almost 3.8 keV for m/z 600.^{32–34} The kinetic energies of negative ions of $m/z > 350$ are sufficiently large that these ions can overcome the potential barrier created by the usual imposition of -1800 V on the detector and give rise to ion signals.¹⁶ Under these conditions, the ratio of signals due to positive ions to those due to negative ions

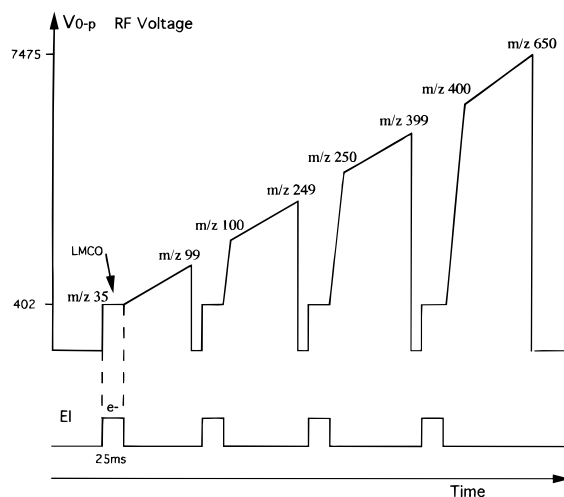


Figure 1. A scan function showing the four segments of the analytical ramp as used for the detection of positive and negative ions. The ionization period was held constant at 25 ms; LMCO is the low-mass cut-off as determined by the magnitude V_{0-p} of the drive potential applied to the ring electrode.

does not reflect the ratio of such ions exiting the ion trap as the response of the detector to negative ions is impaired. Nevertheless, negative ions can be detected, albeit with low efficiency.

RESULTS AND DISCUSSION

Experiments are described in which space charge due mainly to positive ions of low mass/charge ratio perturbs the storage of positive ions of high mass/charge ratio leading to the ejection of positive ions and, consequently, isolation of negative ions of high mass/charge ratio.

The relative abundances of the fragment ion components observed in the EI mass spectrum of FC-43, as employed in the normal ion trap mass calibration procedure, are given in Table 1.

The EI mass spectrum of FC-43, obtained under conditions of abnormally high pressure of FC-43 and with an FEC of 80 μA , is shown in Fig. 2; the mass spectrum

is displayed at low signal amplification. In the inset is shown the region of high mass/charge ratio at high signal amplification so as to show clearly the negative ions at m/z 452, 595 and 633.

Under these ionizing conditions, the positive ions of low mass/charge ratio in Fig. 2 are observed as broad peaks extending over several thomsons, while the positive ions of $m/z > 300$ are either not detected or observed with very weak signal intensity. The broadening of the peak width to several thomsons and the distortion of the peak position towards higher mass/charge ratios are manifestations of space charge perturbations brought about by multitudinous ion-ion interactions of $> 10^5$ positive ions confined simultaneously.²⁹ The decrease in resolution is due to the ejection of ions over a range of higher than normal r.f. amplitudes. This effect is most pronounced for those ions of lowest mass/charge ratio as such ions experience the greatest perturbation upon mass-selective axial ejection. Once ions of low mass/charge ratio have been ejected, the perturbation diminishes and the mass-selective ejection of ions of higher mass/charge ratio becomes less and less affected.

Table 1. Elemental composition and relative abundance of positive ions produced from FC-43, $\text{N}(\text{C}_4\text{F}_9)_3$, under conventional EI conditions and as used for ion trap mass calibration

	69	131	219	264	m/z 414	464	502	614
Structure	CF_3^+	C_3F_5^+	C_4F_9^+	$\text{C}_5\text{F}_{10}\text{N}^+$	$\text{C}_8\text{F}_{16}\text{N}^+$	$\text{C}_9\text{F}_{18}\text{N}^+$	$\text{C}_9\text{F}_{20}\text{N}^+$	$\text{C}_{12}\text{F}_{24}\text{N}^+$
Relative abundance (%)	100	62	31	28	13	2.5	13	2

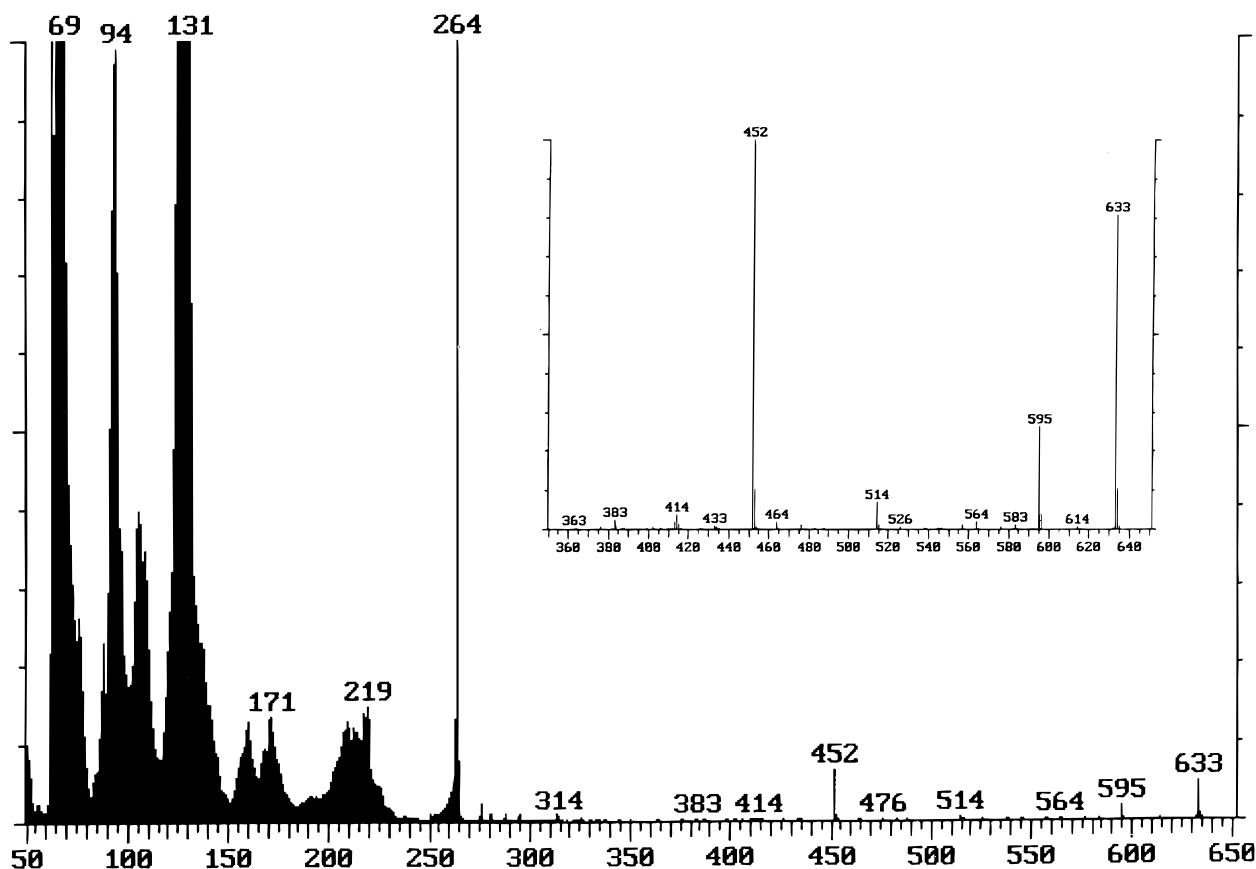


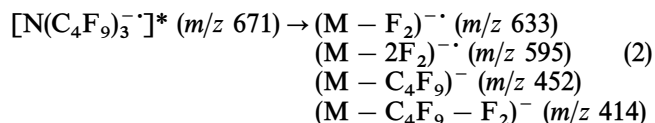
Figure 2. EI mass spectrum of FC-43 acquired under conditions of high space charge and low signal magnification; FEC of 80 μA , LMCO of 35 Th. In the inset is shown the region of high mass/charge ratio at high signal amplification.

The absence of positive ions of $m/z > 200$ from FC-43 in the mass spectrum in Fig. 2 (that is, m/z 264, 464, 502 and 614) indicates that the storage potential for these ion species is highly perturbed. On the other hand, negative ions at m/z 452, 595 and 633, albeit of low signal intensity, are seen clearly in Fig. 2. The empirical formulae of the negative ions are given in Table 2; it should be noted that positive ions characterized by these mass/charge ratios are not observed from FC-43. The polarity of each of the negative ions listed in Table 2 has been verified in a separate experiment³⁴. [A venetian blind type of conversion dynode has been incorporated with the mass spectrometer and inserted between the channeltron electron multiplier and the neighbouring end-cap electrode; variation of the applied to the dynode (-4000 to $+4000$ V) permits the attribution of the polarity of ions ejected from the ion trap]. Moreover, Catinella *et al.*¹⁶ have isolated these ion species with a d.c. isolation sequence in which all positive ions were ejected prior to the analytical scan.

In the formation of positive ions from FC-43 by EI, as is the usual procedure in the ion trap, quasi-thermal electrons are created which may then form the FC-43 molecular negative ion by resonant electron capture, as shown in Eqn (1); it should be noted that the lifetime of the negative molecular ion of m/z 671 is short and it is not detected.¹⁶



Negative ions of m/z 633, 595, 452 and 414 are formed by unimolecular fragmentation of the molecular negative ion, as in Eqn (2), with the loss of F_2 , $2F_2$, C_4F_9 and $C_4F_9 + F_2$, respectively.



Interpretation of the destabilization of positive ion storage

Under conditions of prolonged ionization and/or high sample pressure such that large numbers of ions are accumulated and stored simultaneously in an ion trap, coulombic repulsions among ions of the same polarity induce a space charge potential which can perturb ion motion. When the stored ions are of only a single

species, the manifestations of space charge perturbations are twofold: first, the secular frequencies of ion axial and radial motion are changed and, second, there is a limit, N_{\max} , to the number of ions which can be stored under a given set of trapping conditions. When two or more species are stored simultaneously, a third perturbation is manifested, that of selective ion ejection where the space charge perturbation due to one ion species can neutralize, in part or in whole, the trapping potential for a second ion species of higher mass/charge ratio.

It was over 20 years ago that Schwebel *et al.*²⁶ proposed that the storage of ions within an ion trap could be destabilized by space charge perturbations. Qualitatively, the effect of the space charge perturbation on the stability of ion trajectories can be represented by a translation (to higher q_z values) of the stability diagram boundaries as shown in Fig. 3^{25-27,29} while the q_z values of stored ions are affected less. When the q_z values for ions of high mass/charge ratio no longer reside within the boundaries of the stability diagram, such ions are ejected.

A space charge potential, Φ_S^A , due to coulombic repulsions among positive ions of a single species, A^+ , of mass m_A is added (negatively, as it is repulsive) to the pseudo-potential Φ_0^A that characterizes the main quadrupolar field with respect to A^+ ions. Upon integration of the Mathieu equation with the resulting potential Φ_T , where

$$\Phi_T = \Phi_S^A + \Phi_0^A \quad (3)$$

a modified stability diagram is obtained as shown in Fig. 3. Here, the $\beta_z = 0$ and $\beta_r = 0$ boundaries intersect on the q_z axis at a point q_z^* where $q_z^* > 0$. Indeed, the four boundary limits ($\beta_r = 0, 1$ and $\beta_z = 0, 1$) of the stability diagram are shifted towards higher q_z values.

Parenthetically, let us consider an ion species Y^+ , of mass m_Y and charge $z_Y e$, having the highest mass/charge ratio and lowest q_z value, $q_{z,Y}$, among a number of positive ion species confined simultaneously. Once the space charge perturbed $\beta_r = 0$ and $\beta_z = 0$ boundaries intersect at a point q_z^* such that $q_z^* > q_{z,Y}$, the trajectories of Y^+ ions will no longer be stable and Y^+ ions will be ejected.

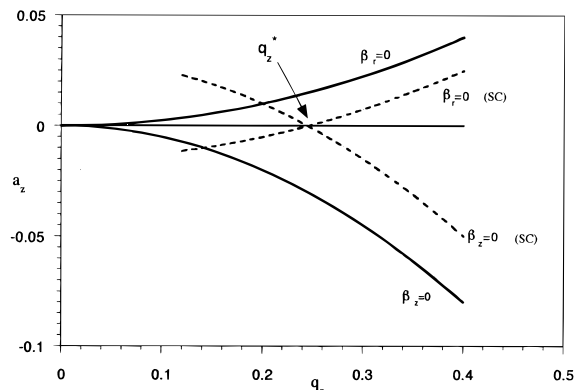


Figure 3. Stability diagram in a_z , q_z space for positive ion storage in a quadrupole ion trap. The dashed line represents the same diagram perturbed by space charge (SC). At the trapping parameter q_z^* , the space charge potential cancels the trapping potential.

Table 2. Elemental composition in the $N(C_n F_{2n+2-x})$ representation of the various negative ion species produced under electron capture conditions

	$n=12$	$n=11$	$n=10$	$n=9$	$n=8$	$n=7$	$n=6$
$x=0$	—	—	—	502 ^a	452	402 ^a	352
$x=1$	633	583	533	483	433	383	—
$x=2$	614	564	514	464	414	364	—
$x=3$	595	545	495	445 ^a	—	—	—
$x=4$	576	526	476	426	—	—	—
$x=5$	557	—	—	407 ^a	—	—	—
$x=6$	538	488 ^a	483 ^a	—	—	—	—
$x=7$	—	469 ^a	—	—	—	—	—

^a Ions of low signal intensity.

The space charge potential Φ_S^A must satisfy the Poisson relationship:

$$\nabla^2 \Phi_S^A = - \frac{n_A z_A e}{\epsilon_0} \quad (4)$$

where n_A and $z_A e$ are the density and charge, respectively, of A^+ and ϵ_0 is the dielectric constant *in vacuo*. As the density n_A increases, the q_z^* value is shifted to higher values and the Φ_S^A potential reduces further the resulting potential, Φ_T , until a maximum ion density, $n_{A, \max}$, is reached when

$$-\nabla^2 \Phi_S^A = \nabla^2 \Phi_0^A \quad (5)$$

Schwebel *et al.*²⁶ expressed the value of $n_{A, \max}$ as

$$n_{A, \max} = \frac{3}{16} \epsilon_0 m_A \left(\frac{\Omega q_{z, A}}{z_A e} \right)^2 \quad (6)$$

where Ω is the angular frequency of the r.f. drive potential and $q_{z, A}$ is the trapping parameter for A^+ ions. McLuckey and co-workers³⁵ used Eqn (6) to estimate the ion density in an ion trap filled of a reactant ion. Todd *et al.*²⁷ and more recently Guan and Marshall³⁰ have expressed the value for $n_{A, \max}$ using the pseudo-potential well-depth approach³⁶ such that

$$n_{A, \max} = \frac{\epsilon_0}{z_A e} \left(D_{r, A} \frac{4}{r_0^2} + D_{z, A} \frac{2}{z_0^2} \right) \quad (7)$$

where r_0 is the radius of the ring electrode, $2z_0$ is the separation distance of the two end-cap electrodes along the z -axis and $D_{r, A}$ and $D_{z, A}$ represent the pseudo-potential well depths in the radial and axial directions, respectively, for A^+ .

This treatment can be extended to the case of several ion species stored simultaneously such that $n_{A, \text{eject}}$ is the density of A^+ necessary for the complete ejection of an ion species Y^+ of higher mass/charge ratio. In this case, $D_{r, Y}$ and $D_{z, Y}$ represent the pseudo-potential well depths in the radial and axial directions, respectively, for Y^+ and are given by

$$D_{r, Y} = \frac{m_Y r_0^2}{2z_Y e} \left(\frac{\Omega}{2} \right)^2 \left(- \frac{a_{z, Y}}{2} + \frac{q_{z, Y}^2}{8} \right) \quad (8)$$

and

$$D_{z, Y} = \frac{m_Y z_0^2}{2z_Y e} \left(\frac{\Omega}{2} \right)^2 \left(a_{z, Y} + \frac{q_{z, Y}^2}{2} \right) \quad (9)$$

where $a_{z, Y}$ and $q_{z, Y}$ are the trapping parameters for Y^+ ions. Substituting for $D_{r, Y}$ and $D_{z, Y}$ in Eqn (7), one obtains

$$n_{A, \text{eject}} = \frac{3}{16} \frac{\epsilon_0 m_Y \Omega^2 q_{z, Y}^2}{z_A z_Y e^2} \quad (10)$$

Equation (10) expresses the conditions $q_z^* = q_{z, Y}$ and yields an estimation of the density of A^+ necessary to eject first ions of the highest mass/charge ratio, Y^+ , then of the higher densities of A^+ necessary to eject ions W^+ , V^+ , etc., in order of decreasing mass/charge ratio. Equation (10) can be rearranged to

$$n_{A, \text{eject}} = \alpha (q_{z, Y})^2 \frac{m_Y}{z_Y} \quad (11)$$

where

$$\alpha = \frac{3}{16} \frac{\epsilon_0 \Omega^2}{z_A e^2}$$

From Eqn (11), it is seen that the density $n_{A, \text{eject}}$ required to destabilize completely the set of ions Y^+ , W^+ , V^+ , etc., is proportional to the product of the mass/charge ratio of each destabilized ion species and the square of the corresponding q_z value.

Space charge destabilization of the trajectories of positive ions

In order to verify the validity of Eqn (11), the ion signal intensities of fragment ions produced by EI of FC-43 were investigated as a function of the filament emission current, I . With a relatively high sample pressure and LMCO of 35 Th, I was varied from 0 to 50 μA . Under these experimental conditions, the abundances of two positive ion species of low mass/charge ratio, m/z 69 and 131, dominated those of the other fragment ion species. Thus, as a first approximation, it was assumed that the m/z 69 and 131 species were responsible for the space charge potential which would bring about the ejection of ions of higher mass/charge ratio. As the observed signal intensities of m/z 69 and 131 increase linearly with I , as shown in Fig. 4, it was assumed that the behavior of the cumulative space charge due to these species as I was increased would parallel that of the space charge due to A^+ as n_A was increased (see above). Hence the magnitude of $n_{A, \text{eject}}$ can be assumed to be directly proportional to the number of A^+ ions created and stored in the ion trap which, in turn, is directly proportional to I . This assumption is justified when the distributions of ions in space is uniform, that is, when the density is constant.

Such a distribution is not realistic for a quadrupole ion trap with a helium buffer gas pressure of *ca.* $\sim 10^{-3}$ Torr such that the ion cloud can become focused near the center of the ion trap. Nevertheless, Todd *et al.*²⁷ have shown that Eqn (6) can be verified experimentally when the value of n_A is assumed to be proportional to the duration of ionization at constant I . This observation supports the assumption that, to a first approximation, the density n_A is proportional to the number of

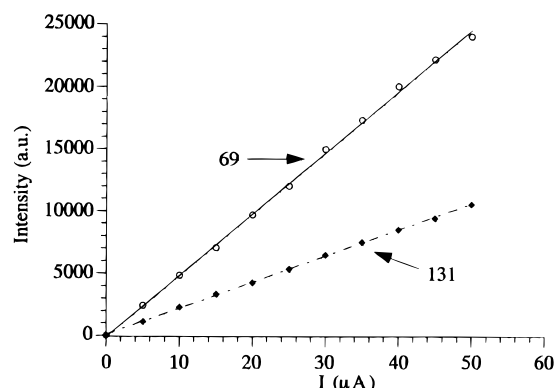


Figure 4. Variations of the positive ion signal intensities of m/z 69 and 131 with filament emission current, I ; LMCO of 35 Th. High space charge conditions were encountered at the upper range of I .

A^+ ions created and, thus, is related linearly to the filament emission current, I , at a constant duration of ionization.

The evolution of the signal intensities of three positive ion species, m/z 464, 502 and 614, as a function of I is shown in Fig. 5.

For each of the positive ions, the signal intensity was integrated over several mass/charge units as the mass resolution deteriorated due to space charge at the higher values of I investigated. Initially, the ion signal intensity increased with I until, as the density of low mass/charge ratio ions increased, the trajectories of the high mass/charge ratio ions became unstable owing to the space charge potential; the signal intensity reached a plateau, then decreased to a negligible value. For example, the signal intensity of m/z 614 decreased to a negligible value at $I = 20 \mu\text{A}$, which was designated I_{eject} ; the I_{eject} values for m/z 502 and 464 were 24.5 and 28 μA , respectively.

Additional values of I_{eject} were determined for the ejection of each of the ion species of m/z 576, 564, 514, 426, 414, 364 and 314. All of the data are plotted in Fig. 6; here, the plot of $m_{\text{Y}}/z_{\text{Y}}$ (left-hand ordinate) versus I_{eject} shows inverse proportionality in that the ions were ejected in order of descending mass/charge ratio as

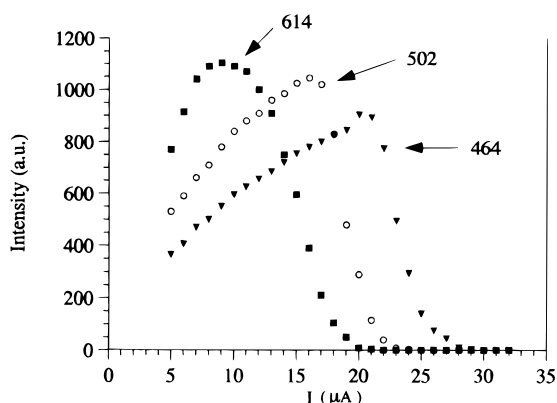


Figure 5. Variations of the positive ion signal intensities of m/z 464, 502 and 614 with filament emission current, I ; LMCO of 35 Th. High space charge conditions were encountered by each species leading to total ion ejection.

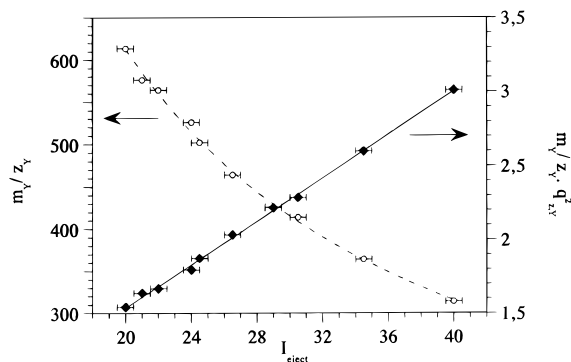


Figure 6. Successive ejection of positive ions of high mass/charge ratio with increasing space charge potential; LMCO of 35 Th. Left-hand ordinate, variation of $m_{\text{Y}}/z_{\text{Y}}$ versus I_{eject} ; right-hand ordinate, $q_{z,\text{Y}}^2 m_{\text{Y}}/z_{\text{Y}}$ versus I_{eject} , as per Eqn (10). The data plotted are for the positive ion species of m/z 576, 564, 514, 502, 464, 426, 414, 364 and 314.

expected, while the linear plot of $q_{z,\text{Y}}^2 m_{\text{Y}}/z_{\text{Y}}$ (right-hand ordinate) versus I_{eject} shows that Eqn (11) is obeyed. It should be noted that, as $q_{z,\text{Y}}$ is inversely proportional to $m_{\text{Y}}/z_{\text{Y}}$, $q_{z,\text{Y}}^2 m_{\text{Y}}/z_{\text{Y}}$ is proportional to $z_{\text{Y}}/m_{\text{Y}}$.

The linearity of the plot of $q_{z,\text{Y}}^2 m_{\text{Y}}/z_{\text{Y}}$ versus I_{eject} appears to confirm the assumption made concerning the cumulative space charge effect exerted by the two ions of low mass/charge ratio, m/z 69 and 131, and that the relatively simple theoretical approach to the neutralization of trapping potentials is justified. Furthermore, the value of $n_{\text{A,max}}$ can be estimated from Eqn (10): for an LMCO of 35 Th corresponding to an r.f. voltage amplitude of 402 V_{0-p} , with $\Omega/2\pi = 1.05 \text{ MHz}$, $\epsilon_0 = 8.85 \times 10^{-12} \text{ F m}^{-1}$ and $e = 1.6 \times 10^{-19} \text{ C}$, the calculated value for $n_{\text{A,max}}$ was found to lie in the range $0.7\text{--}1.4 \times 10^7 \text{ ions cm}^{-3}$ for the ejection of positive ions over the mass/charge ratio range from 614 to 314. The range of ion densities calculated here is in good agreement with other estimations and, in particular, with the maximum ion density.^{25,26,37-39}

Ejection of positive ions concurrent with negative ion detection

In the experiment described above, the abundance of positive ions of high mass/charge ratio is reduced dramatically for values of I greater than 10–20 μA , as shown in Fig. 5; however, additional ion signals were observed and have been ascribed to negative ions of m/z 452 ($[\text{M} - \text{C}_4\text{F}_9]^-$), m/z 595 ($[\text{M} - 2\text{F}_2]^-$), m/z 633 ($[\text{M} - \text{F}_2]^-$) and m/z 414 ($[\text{M} - \text{C}_4\text{F}_9 - \text{F}_2]^-$). These ions are the most abundant species in the mass spectrum shown in Fig. 2 and have kinetic energies which are sufficiently large to permit their detection with a channeltron biased at $\sim -1800 \text{ V}$. All other negative ions were observed with lower abundance and have been interpreted as reported in Table 2. No negative ions were detected with $m/z < 350$.

The observation of negative ions, e.g. m/z 595 and 633 as shown in Fig. 7(a) and (b), respectively, requires a threshold FEC of $\sim 15 \mu\text{A}$, at which point positive ions of high mass/charge ratio have been ejected either almost entirely or in part.

The ion signal intensities for negative ions of m/z 595 and 633 increase relatively rapidly from $I = 15$ to 22 μA ; thereafter, the slope of the signal intensity as a function of I decreases to a value which extrapolates back to a point close to the origin. These observations suggest that the behavior of negative ions is subject to two different influences. First, for $I < 22 \mu\text{A}$, it is proposed that the negative ion abundance can be limited by ion–ion recombination of positive ions and negative ions of similar mass/charge ratio; such ions experience similar regions of space in the ion trap, have similar secular frequencies and ion–ion recombination will be favored when their kinetic energies are simultaneously low. Second, for $I > 22 \mu\text{A}$, the trajectories of positive ions of high mass/charge ratio are destabilized by the accumulated space charge potential so that these ions are ejected; ion–ion recombination is no longer possible and the signal intensities of the negative ions of m/z 595 and 633 show linear increases with increasing I . The linearity of the dashed lines is interpreted as evidence in

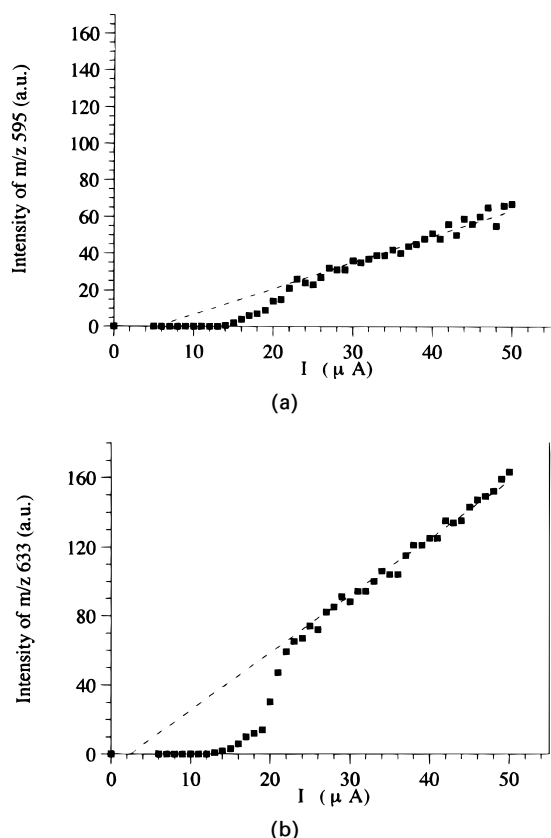


Figure 7. Variation of (a) the m/z 595 and (b) the m/z 633 negative ion signal intensity with filament emission current I . Note that at the value of I for the disappearance of neighboring positive ions (Fig. 5), the slope of the negative ion signal intensity increases rapidly. The dashed lines at low I show the estimated negative ion signal intensities in the absence of positive ions of high mass/charge ratio. Positive ions of low mass/charge ratio are present throughout, as in Fig. 5.

support of a lack of ion-ion recombination of positive ions of low mass/charge ratio with negative ions of high mass/charge ratio.

The conditions of high space charge, where positive ions of high mass/charge ratio are ejected, are the optimum conditions for the detection of high mass/charge ratio negative ions of m/z 452, 595 and 633. While the observation of these negative ion species is not in itself evidence of an enhancement of the storage potential (as opposed to a null effect), the pseudo-potential well-depth experienced by negative ions appears to be enlarged by positive space charge. Consider the following two experiments in which the effects on FC-43 negative ion signal intensities of removing positive ions were examined. In each experiment, the LMCO during ionization was 10 Th, the FEC was 20 μ A and the duration of ionization was 25 ms; under these conditions, the trapping potential for positive ions of high mass/charge ratio ($m/z > 200$) was reduced (to about one quarter of that for an LMCO of 35 Th).

The scan function for the first experiment is given in Fig. 8(a) and shows a period of ionization, A, followed by a period of cooling or storage, B, prior to the mass-selective analytical scan. For the second experiment, the scan function used is given in Fig. 8(b) and is a modified version of that in Fig. 8(a); it includes a ramp of the r.f. voltage amplitude, B, such that all ions of $m/z < 400$

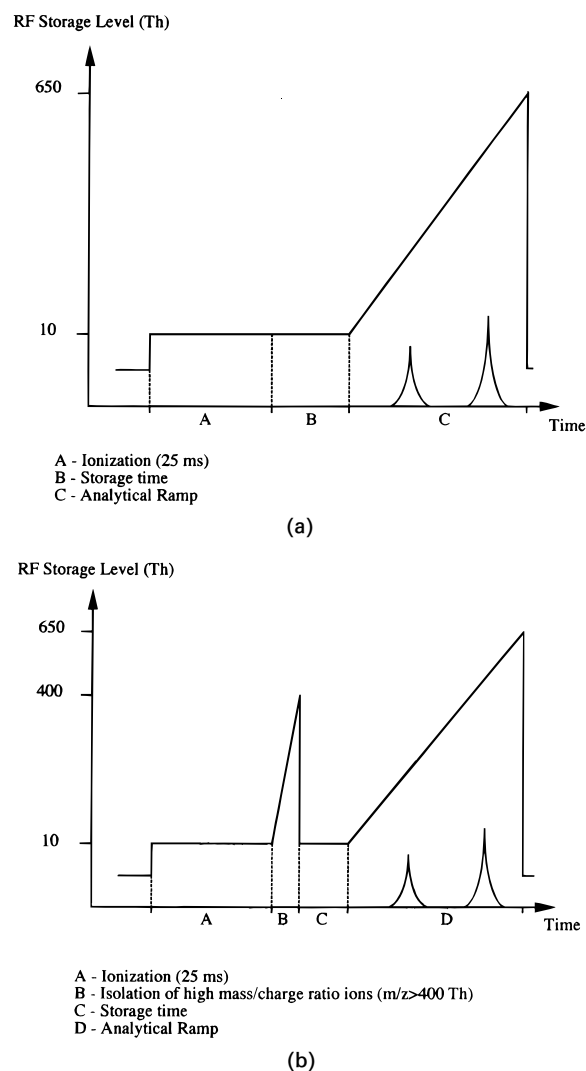


Figure 8. (a) Scan function 1 for the simultaneous confinement of high mass/charge ratio negative ions and low mass/charge positive ions with a storage period of variable duration following ionization; high mass/charge ratio positive ions were ejected by space charge during the ionization period. (b) Scan function 2 for the isolation of high mass/charge ratio negative ions ($m/z > 400$) with a storage period of variable duration following isolation; high mass/charge ratio positive ions were ejected by space charge during the ionization period and all ions of $m/z < 400$ were ejected during period B.

were ejected immediately following ionization, A, and prior to the storage period, C. The first experiment yielded a plot of the resulting signal intensity of the negative ion of m/z 452 ($q_z = 0.013$) versus the duration of the storage period B and is shown in Fig. 9(a); during the first 50 ms of storage, the signal intensity meanders somewhat but the overall decrease is $< 15\%$, and thereafter the signal intensity is reduced to $\sim 1\%$ at 80 ms and is negligible at 100 ms. The second experiment yielded the variation of the signal intensity of the same negative ion of m/z 452 versus the duration of the storage period C [Fig. 9(b)]; it is seen that the signal intensity falls to zero in 1.4 ms.

From a comparison of the traces in Fig. 9(a) and (b), noting that the abscissa scales differ by a factor of 75, the storage of negative ions at low q_z values appears to be enhanced when such ions are confined simultaneously with positive ions of low mass/charge ratio.

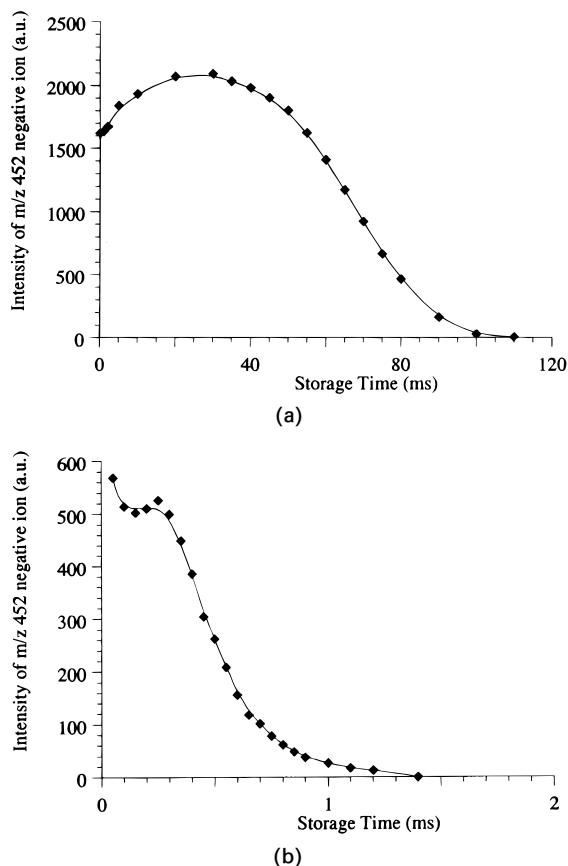


Figure 9. Variation of the m/z 452 negative ion signal intensity with storage time at $q_z = 0.013$ using scan function (a) 1 and (b) 2.

Such behavior is complementary to the storage impairment of ion storage or ion ejection of high mass/charge ratio positive ions when such ions are confined simultaneously with positive ions of low mass/charge ratio. As the space charge potential created by positive ions of low mass/charge ratio decreases the trapping potential well for positive ions with low q_z values, the trapping potential well is increased for negative ions with similarly low q_z values. In this latter case, the space charge potential, Φ_S^A , is added to Φ_0 in Eqn (3) with the result that the potential well depths, D_{r, Y^-} and D_{z, Y^-} , for Y^- ions given by Eqns (8) and (9), respectively, are increased.

CONCLUSION

A simple theoretical treatment has been presented of space charge perturbation of the trapping potential exhibited when positive ions in the range m/z 69–614 are confined simultaneously in a quadrupole ion trap. The trapping potentials for ions of high mass/charge ratio with q_z in the range 0.05–0.1 are much smaller than those for ions of low mass/charge ratio and can be neutralized by increased accumulation of ions of low mass/charge ratio. Neutralization of the trapping potential leads to ion ejection. With increasing density of ions of low mass/charge ratio, ions of the highest mass/charge ratio are ejected first and are followed by other species in descending order of mass/charge ratio. A simple relationship between ion density and the mass/charge ratio of the ejected ion species has been derived and demonstrated experimentally.

The ejection of positive ions of high mass/charge ratio permits unobscured observation of negative ions of high mass/charge ratio which possess sufficient kinetic energy upon mass-selective axial ejection to overcome the ~ -1800 V bias on the detector. The variation of negative ion signal intensities with low filament emission current ($< 22 \mu\text{A}$) has been interpreted in terms of ion–ion recombination with positive ions of high mass/charge ratio. The linearity of negative ion signal intensities with high filament emission current ($> 22 \mu\text{A}$) has been interpreted in terms of reduced ion–ion recombination of negative ions with positive ions of low mass/charge ratio which, although present in abundance, occupy different regions of space within the ion trap.

The observation of storage impairment for positive ions of high mass/charge ratio by positive ions of low mass/charge ratio is complementary to the observation of storage enhancement for negative ions of high mass/charge ratio also by positive ions of low mass/charge ratio.

Acknowledgements

The authors thank the Centre d'Etudes du Bouchet, Université Pierre et Marie Curie and CNRS for financial support. The technical support of Varian-France and Varian Associates is acknowledged gratefully. R. E. M. acknowledges the support of the Natural Sciences and Engineering Research Council (NSERC) of Canada and the NSERC of Canada Industrially-Oriented Research Program.

REFERENCES

1. J. H. Bowie, *Mass Spectrom. Rev.* **3**, 161 (1984).
2. S. V. Ong and R. A. Hites, *Mass Spectrom. Rev.* **13**, 259 (1994).
3. R. C. Dougherty, *Anal. Chem.* **53**, 625A (1981).
4. J.-C. Tabet, in *Fundamentals of Gas Phase Ion Chemistry*, edited by K. R. Jennings, p. 351. Kluwer, Dordrecht (1992).
5. R. E. March and R. J. Hughes, *Quadrupole Storage Mass Spectrometry*, Chemical Analysis Series, Vol. 102. Wiley, New York (1989).
6. B. D. Nourse and R. G. Cooks, *Anal. Chim. Acta* **3**, 228 (1990).
7. R. E. March and J. F. J. Todd (Eds), *Practical Aspects of Ion Trap Mass Spectrometry*, Vols. 1–3. CRC Press, Boca Raton, FL (1995).
8. O. D. Sparkman and R. D. Brittain, in *Proceedings of the 42nd ASMS Conference on Mass Spectrometry and Allied Topics*, Chicago, IL, 1994, p. 700.
9. J. B. Plomley, R. S. Mercer and R. E. March, in *Proceedings of the 43rd ASMS Conference on Mass Spectrometry and Allied Topics*, Atlanta, GA, 1995, p. 230.
10. J. B. Plomley, C. J. Koester, M. Lausevic, X. Jiang, F. A. Londry and R. E. March, in *Proceedings of the 43rd ASMS Conference on Mass Spectrometry and Allied Topics*, Atlanta, GA, 1995, p. 993.
11. J.-P. Schermann and F. G. Major, *Appl. Phys.* **16**, 225 (1978).
12. R. E. Mather and J. F. J. Todd, *Int. J. Mass Spectrom. Ion Phys.* **33**, 159 (1980).
13. D. W. Berberich and R. A. Yost, *J. Am. Soc. Mass Spectrom.*

- 5, 757 (1994).
14. S. A. McLuckey, G. L. Glish and P. E. Kelley, *Anal. Chem.* **59**, 1674 (1987).
 15. R. E. Pedder and R. A. Yost, in *Proceedings of the 36th ASMS Conference on Mass Spectrometry and Allied Topics*, San Francisco, CA, 1988, p. 632.
 16. S. Catinella, P. Traldi, X. Jiang, F. A. Londry, R. J. S. Morrison, R. E. March, S. Gregoire, J.-C. Mathurin and J.-C. Tabet, *Rapid Commun. Mass Spectrom.* **9**, 1302 (1995).
 17. J.-C. Mathurin, S. Gregoire, A. Brunot, J.-C. Tabet and R. E. March, in *Proceedings of the 44th ASMS Conference on Mass Spectrometry and Allied Topics*, Portland, OR, 1996, p. 144.
 18. K. G. Asano, G. L. Glish and S. A. McLuckey, in *Proceedings of the 36th ASMS Conference on Mass Spectrometry and Allied Topics*, San Francisco, CA, 1988, p. 636.
 19. S. A. McLuckey, K. G. Asano and G. L. Glish, in *Proceedings of the 36th ASMS Conference on Mass Spectrometry and Allied Topics*, San Francisco, CA, 1988, p. 1108.
 20. C. A. Valkenburg, L. A. Krieger and E. P. Grimsrud, *J. Chem. Phys.* **86**, 6782 (1987).
 21. S. A. McLuckey, G. L. Glish and K. G. Asano, *Anal. Chim. Acta* **229**, 25 (1989).
 22. B. A. Eckenrode, G. L. Glish and S. A. McLuckey, *Int. J. Mass Spectrom. Ion Processes* **99**, 151 (1990).
 23. G. J. Van Berkel, G. L. Glish and S. A. McLuckey, *Anal. Chem.* **62**, 1284 (1990).
 24. J. D. Williams and R. G. Cooks, *Rapid Commun. Mass Spectrom.* **7**, 380 (1993).
 25. E. Fisher, *Z. Phys.* **156**, 1 (1959).
 26. C. Schwebel, P. A. Moller and P. T. Manh, *Rev. Phys. Appl.* **10**, 227 (1975).
 27. J. F. J. Todd, R. M. Waldren and R. E. Mather, *Int. J. Mass Spectrom. Ion Phys.* **34**, 325 (1980).
 28. J. F. J. Todd, R. M. Waldren, D. A. Freer and R. B. Turner, *Int. J. Mass Spectrom. Ion Phys.* **35**, 107 (1980).
 29. F. Vedel and J. André, *Int. J. Mass Spectrom. Ion Processes* **65**, 1 (1985).
 30. S. Guan and A. G. Marshall, *J. Am. Soc. Mass Spectrom.* **5**, 64 (1994).
 31. J. H. Parks and A. Szöke, *J. Chem. Phys.* **103**, 1422 (1995).
 32. R. E. March, A. W. McMahon, E. T. Allison, F. A. Londry, R. L. Alfred, J. F. J. Todd and F. Vedel, *Int. J. Mass Spectrom. Ion Processes* **99**, 109 (1990).
 33. H. P. Reiser, R. E. Kaiser, P. J. Savickas and R. G. Cooks, *Int. J. Mass Spectrom. Ion Processes* **106**, 237 (1991).
 34. S. Gregoire, J.-C. Mathurin, A. Brunot, R. E. March and J.-C. Tabet, to be published.
 35. W. J. Herron, D. E. Goeringer and S. A. McLuckey, *J. Am. Soc. Mass Spectrom.* **6**, 529 (1995).
 36. H. G. Dehmelt, *Adv. At. Mol. Phys.* **3**, 53 (1967).
 37. J. E. Fulford, D.-N. Hoa, R. J. Hughes, R. E. March, R. F. Bonner and G. J. Wong, *J. Vac. Sci. Technol.* **17**, 829 (1980).
 38. M. N. Gaboriaud, M. Desaintfuscien and F. G. Major, *Int. J. Mass Spectrom. Ion Phys.* **41**, 109 (1981).
 39. E. P. Sheretov, V. A. Zenkin and V. F. Samodurov, *Sov. Phys. Tech. Phys.* **18**, 282 (1973).